Chem. Senses 35: 239–245, 2010
doi:10.1093/chemse/bjq007
Advance Access publication January 25, 2010

# Tmem16b is Specifically Expressed in the Cilia of Olfactory Sensory Neurons

**Sebastian Rasche[1], Bastian Toetter[1], Jenny Adler[2], Astrid Tschapek[2], Julia F. Doerner[1], Stefan Kurtenbach[1], Hanns Hatt[1], Helmut Meyer[2], Bettina Warscheid[2] and Eva M. Neuhaus[3]**

[1]Department of Cell Physiology, Ruhr-University Bochum, Universitaetsstrasse 150, 44780 Bochum, Germany, [2]Medical Proteome Center, Ruhr-University Bochum, Universitaetsstrasse 150, 44780 Bochum, Germany and [3]NeuroScience Research Center, Charité, Charitéplatz 1, 10117 Berlin, Germany

*Correspondence to be sent to: Eva M. Neuhaus, NeuroScience Research Center, Charité, Universitätsmedizin Berlin, 10117 Berlin, Germany. e-mail: eva.neuhaus@charite.de*

*Accepted January 7, 2010*

## Abstract

Calcium-activated chloride channels (CaCCs) are involved in many physiological processes, including sensory signal transduction, but only little is known to date about their structure and function. We performed a proteome analysis of the olfactory epithelium (OE) membrane proteome and identified so far uncharacterized membrane proteins as candidate channels. One of the most abundant membrane proteins in olfactory sensory neurons (OSNs) was Tmem16b, a member of a recently identified family of CaCCs. In addition to former studies performed on Tmem16b, we show here that Tmem16b expression is highly specific for the OE, in contrast to the closely related Tmem16a, which shows a broad expression pattern in secretory epithelial cells. Native Tmem16b is localized in the cilia of the OSNs, which is in agreement with previous electrophysiological recordings.

**Key words:** chloride channel, proteomics, signal transduction, Tmem16b

## Introduction

The responses of olfactory sensory neurons (OSNs) to odorant stimuli consist of 2 main currents, a small $Ca^{2+}$ influx mediated by cyclic nucleotide gated (CNG) channels and a strong $Cl^-$ efflux, that is mediated by a calcium-activated chloride channel (CaCC). This CaCC belongs to the family of chloride channels that are regulated by the cytosolic $Ca^{2+}$ concentration. The membrane conductance induced by this CaCC is large enough to profoundly affect electrical excitability of the neurons (Frings et al. 2000; Reisert et al. 2005), and the channel was shown to be expressed in the cilia of OSNs by electrophysiological methods. The molecular identity of this channel was unknown for long time. Bestrophin-2 has been described as a candidate (Pifferi et al. 2006), but bestrophin-2 knockout mice showed neither deficits in a behavioral assay of olfactory function (Bakall et al. 2008) nor significantly different responses to odorant stimuli compared with wild type mice (Pifferi et al. 2009).

Recently, a new protein family of CaCCs, the anoctamin/Tmem16 family, has been described (Caputo et al. 2008; Schroeder et al. 2008; Yang et al. 2008). Expression of these genes was previously found to be implicated in gnathodiaphyseal dysplasia (Tsutsumi et al. 2005) and in some forms of cancer (Huang et al. 2006), but their function was unknown. The Tmem16 family members have 8 predicted transmembrane segments and a conserved C-terminal domain of unknown function named DUF590. Tmem16a, the first characterized family member, has been shown to be activated by receptors that elevate intracellular $Ca^{2+}$ (Schroeder et al. 2008; Yang et al. 2008) and by intracellular $Ca^{2+}$ release mediated by photolysis of caged Inositol-1,4,5-trisphosphat (Schroeder et al. 2008; Yang et al. 2008). Tmem16a is expressed in many of the tissues that are known to express CaCCs, such as bronchiolar epithelial cells, pancreatic acinar cells, proximal kidney tubule epithelium, retina, dorsal root ganglion sensory neurons, and submandibular gland (Caputo et al. 2008; Schroeder et al. 2008; Yang et al. 2008).

Tmem16b, a second member of the anoctamin/Tmem16 family, has also been shown to act as a CaCC (Schroeder et al. 2008; Pifferi et al. 2009; Stephan et al. 2009; Stohr et al. 2009). Interestingly, heterologously expressed Tmem16b exhibits channel properties similar to the native olfactory CaCC (Stephan et al. 2009), indicating a possible

involvement of Tmem16b in the olfactory signal transduction cascade. Although trafficking of an overexpressed Tmem16b::enhanced green fluorescent protein (EGFP) fusion protein to olfactory cilia has been shown (Stephan et al. 2009), the localization of endogenous Tmem16b in the olfactory epithelium (OE) and in other tissues is still unknown.

We performed quantitative proteomics analysis of the membrane proteome of cilia preparation from OE and identified several so far unknown membrane proteins, among them Tmem16b. We report here that endogenous Tmem16b is specifically expressed in the cilia of OSNs and could detect exactly the stoichiometry of CNG channel subunits and Tmem16b to explain earlier electrophysiological results.

## Materials and methods

### Antibodies and chemicals

Acetonitrile (ACN) (high-performance liquid chromatography [HPLC]-S gradient grade) was purchased from Biosolve, formic acid (FA) from J.T. Baker B.V., trifluoroacetic acid from Merck, sequencing grade modified trypsin from Promega, dextran T500 from Carl Roth, and polyethylenglycol (PEG) 3350 from Fluka. Anti-acetylated tubulin antibody was from Sigma, anti-CNGA2 from Santa Cruz, fluorescent secondary antibodies were from Invitrogen, and horseradish peroxidase coupled secondary antibodies were from Biorad. Tmem16b antibody was generated against an epitope of the intracellular C-terminus with the following unique sequence motif: VKLADEPTQRSQG, Rabbits were immunized with peptides by Eurogentec.

### Immunohistochemistry

Immunostaining was done on 10-μM coronal cryosections of paraformaldehyde-fixed tissue on superfrost slides (Menzel), HEK293 cells were grown on coverslips (80–100 μm; Menzel Gläser) and fixed in paraformaldehyde. Sections and cells were incubated with antibodies in phosphate-buffered saline/gelatin/Triton X-100 and mounted in ProLong Antifade (Molecular Probes). Fluorescence images were obtained with a confocal microscope (Leica) and further processed with Photoshop (Adobe Systems Inc.).

### Preparation of plasma membranes and olfactory cilia from mice

For cilia enrichment, the cilia were dislodged from the OE using the calcium shock method, and 10 μg total protein was subjected to 1-D polyacrylamide gel electrophoresis (PAGE). In independently performed plasma membrane preparations, mouse OE was homogenized using pestle and mortar in an aqueous 2-phase system consisting of 6.3% (w/w) PEG, 6.3% (w/w) dextran, 15 mM Tris–$H_2SO_4$ pH 7.8, and 5 mM boric acid. Membrane proteins were incubated with 100 mM $Na_2CO_3$ (pH 11.5/4 °C) for 15 min and centrifuged. Ciliary and plasma membranes were solubilized in Laemmli buffer and applied to a 4–12% or 12% Bis–Tris gels with a 3-(N-Morpholino)-Propansulfonsäure buffer system (NUPAGE-Novex, Invitrogen).

### SDS-PAGE and in-gel digestion

For proteomics analysis of ciliary membranes and plasma membranes of the OE, sodium dodecyl sulfate (SDS)-gels were stained by colloidal coomassie brilliant blue G-250. The gel was equally cut in 2 mm slices. Gel bands were destained by alternately incubating them with 20 μL of 10 mM ammonium hydrogencarbonate ($NH_4HCO_3$) and 20 μL of 5 mM $NH_4HCO_3$/50% ACN (v/v) for 10 min each. Gel pieces were dried in vacuo, and proteins were digested in gel applying 2-μL trypsin solution (0.03 μg/μL trypsin in 10 mM $NH_4HCO_3$, pH 7.8) overnight at 37 °C. The resulting tryptic peptides were extracted twice with 10 μL of 2.5% FA/50% ACN (v/v); extracts were combined, dried in vacuo, and eventually reconstituted in 15 μL of 5% FA/5% ACN (v/v).

### Mass spectrometry

Tryptic digests were analyzed by nano HPLC/elektrosprayionisation (ESI)-mass spectrometry (MS)/MS using the UltiMate 3000 HPLC system (Dionex LC Packings) online coupled to an linear trap quadrupole (LTQ) Orbitrap XL instrument (Thermo Fisher Scientific). Reversed-phase (RP) capillary HPLC separations were performed as described previously (Schaefer et al. 2004) with slight modifications. In brief, peptide mixtures were loaded onto 1 of 2 C18 μ-precolumns (0.3 mm inner diameter [i.d.] × 5 mm; PepMap, Dionex LC Packings) equilibrated in 0.1% (v/v) trifluoroacetic acid, washed, and preconcentrated for 5 min with the same solvent at a flow rate of 30 μL/min using the loading pump. The precolumn was then switched in line with a C18 RP nano LC column (75 μm i.d. × 150 mm; PepMap, Dionex LC Packings). For peptide separation, a binary solvent system consisting of 0.1% (v/v) FA (solvent A) and 0.1% (v/v) FA/84% (v/v) ACN (solvent B) was applied. The gradient was as follows: 5–50% solvent B in 40 min and 50–95% solvent B in 2 min; the nano LC column was then washed for 3 min with 95% solvent B and subsequently equilibrated for the next run with 5% solvent B (20 min). The flow rate was 150 nL/min.

The LTQ Orbitrap XL instrument was equipped with a nanoelectrospray ion source (Thermo Fisher Scientific) and distal coated SilicaTips (FS360-20-10-D; New Objective). The instrument was externally calibrated using standard components, and lock masses were used for internal calibration. Mass spectrometric parameters were as follows: spray voltage, 1.7–2.0 kV; capillary voltage, 45 V; capillary temperature, 200 °C; and tube lens voltage, 100 V. For data-dependent MS/MS analyses, the software XCalibur 2.0 SR 2 (Thermo Fisher Scientific) was used. MS spectra ranging from m/z 300 to 1500 were acquired in the Orbitrap at a resolution of 30 000 (at m/z 400). Automatic gain control

(AGC) was set to $5 \times 10^5$ ions and a maximum fill time of 750 ms. After a brief survey scan, the 4 most intense multiply charged ions were selected for low energy collision-induced dissociation in the linear ion trap concomitant with the completion of the MS scan in the Orbitrap. The AGC of the LTQ was set to 10 000 ions and a maximum fill time of 100 ms. Fragmentation was carried out at a normalized collision energy of 35% with an activation $q = 0.25$ and an activation time of 30 ms. The fragmentation of previously selected precursor ions was dynamically excluded for the following 45 s.

### Data analysis

Peaklists of MS/MS spectra were generated using the software tools Bioworks 3.1 SR 1 applying default parameters. For peptide and protein identification, peaklists were correlated with the mouse International Protein Index (Mouse IPI v3.30.; Mouse IPI v3.54) (http://www.ebi.ac.uk) MASCOT (release version 2.2.0) (Perkins et al. 1999). All searches were performed with tryptic specificity allowing 2 missed cleavages, and oxidation of methionine and carbamidomethylation were set as variable modifications. Mass spectra were searched with a mass tolerance of 3 ppm for precursor ions and 0.6 Da for fragment ions. Cut-off scores applied in this work provided highest number of protein identifications on the basis of one peptide and a false discovery rate below 5% calculated as described (Stephan et al. 2006; Wiese et al. 2007). Proteins were assembled on the basis of peptide identifications using the ProteinExtractor Tool (version 1.0) in ProteinScape (version 1.3, Bruker Daltonics) and sorted according to their identification scores. Subcellular localizations of proteins were determined via SwissProt (http://ca.expasy.org/) annotation.

### Western blotting

For western blotting, 10 μg of protein was resolved by 8% SDS-PAGE and transferred to nitrocellulose membrane (Protran; Schleicher & Schuell). The nitrocellulose membranes were blocked and incubated with the antibodies diluted in 4% dry milk in tris-buffered saline with tween. Detection was performed with ECL plus (Amersham) on Hyperfilm ECL (Amersham).

### Reverse transcriptase-polymerase chain reaction

RNA of different mouse tissues was isolated with Trizol reagent (Invitrogen), digested with DNAseI (Fermentas), and purified again with Trizol before isolation of polyA+ messenger RNA (mRNA) with oligo-dT-coated paramagnetic particles (Dynal). cDNA was synthesized by using moloney murine leukemia virus reverse transcriptase (Invitrogen) and oligo (dT12-18) primer. Polymerase chain reaction (PCR) was performed with 2-ng template cDNA and specific primer pairs for Tmem16 family members. The primers and expected sizes are given in Supplementary Table 3.

### Cloning of full-length Tmem16b

Mouse Tmem16b was amplified from cDNA from OE by PCR using the primer pair Tmem16b-Fwd (CATGCACTTTCACGACAACCAGAGGAAAGTC) and Tmem16b-Rev (TCATACATTGGTGTGCTGGGACCCTG), which amplify the whole open reading frame (NM_153589). The generated plasmid was verified by sequencing.

### Cell culture and transfection

Reagents for cell culture use were purchased from Invitrogen. HEK293 cells were maintained under standard conditions in Minimum Essential Medium supplemented with 10% fetal bovine serum, 100 units/ml penicillin and streptomycin, and 2 mM L-glutamine. HEK293 cell transfections with the Tmem16b-containing plasmid were performed using a standard calcium phosphate precipitation technique.

## Results

### Mass spectrometry of OE membranes

We employed a highly sensitive (MS)-based proteomics approach to get to quantitative information on the composition of the olfactory membrane proteome in mouse. In total, 1453 and 818 proteins were reliably identified in plasma membranes and ciliary membranes of mouse OE, respectively (Supplementary Tables S1 and S2). About half of the proteins identified in both preparations are annotated as integral membrane proteins comprising numerous proteins with known functions in the olfactory signal transduction cascade, such as adenylate cyclase III and CNGA2, CNGA4, and cyclic nucleotide gated channel B1b (CNGB1b). Because we readily identified membrane components that play key roles in olfaction, we deemed our olfactory membrane proteomics survey to be a valuable tool for the identification of new candidates of CaCCs. We consistently identified 3 proteins belonging to the Tmem16 family (Tmem16a, Tmem16b, and Tmem16f) in both plasma and ciliary membranes of the mouse OE. In addition, we identified membrane proteins for which no functional annotations have been described yet (Tmem30a, 33, 111, 205, 109, and Tmem43). Tmem16a and Tmem16b, also referred to as Anoctamin1 and 2, were reported as bona fide CaCC (Caputo et al. 2008; Schroeder et al. 2008; Yang et al. 2008; Pifferi et al. 2009; Stohr et al. 2009), and Tmem16b (Anoctamin2) has recently been proposed as the CaCC in OSNs (Stephan et al. 2009). Furthermore, we identified 2 additional proteins of the Tmem16 family, Tmem16f and Tmem16k, in olfactory membranes. In addition to former mass spectrometric analysis of the cilia of olfactory neurons in rats (Mayer et al. 2008) and mice (Stephan et al. 2009), we semiquantitatively evaluated the relative abundance of Tmem16 proteins in olfactory membranes on the basis of spectral counts, which reflects the fact that higher abundance

proteins are sampled more frequently (Liu et al. 2004). Tmem16b is significantly more abundant than Tmem16a and about 2-fold more abundant than CNGA2 (Figure 1A). Spectral counts for CNGA2 (39,42), CNGB1b (10,9), and CNGA4 (13,27) were in relative agreement with the 2:1:1 ratio expected for the 3 channel subunits, showing the validity of the quantitative analysis. Abundance of Tmem16f in olfactory membranes appeared to be comparable with the abundance of Tmem16a, whereas Tmem16k was detected in ciliary membranes only. To additionally verify expression of Tmem16b in the mature sensory neurons of the epithelium, we performed reverse transcriptase-PCR (RT-PCR) with fluorescence-activated cell sorting (FACS) sorted OSNs from olfactory marker protein (OMP) green fluorescent protein (GFP) mice (Potter et al. 2001) (Supplementary Figure 1A) and in situ hybridization with OE cryosections (Supplementary Figure 1B), which were in direct agreement with former studies (Stephan et al. 2009).

These data demonstrate that Tmem16b protein is present in adequate amounts in the cilia of OSNs to fulfill the known function in the olfactory signal transduction cascade.

### Expression of Tmem16 family members in OE

To analyze and validate expression of all Tmem16 family members, we performed RT-PCR with OE mRNA using intron-spanning primer pairs that specifically detect the different Tmem16 proteins (Figure 1B). As positive control, we prepared mRNA from tissues where the respective Tmem16 family member is known to be expressed or where we could detect expression by RT-PCR. Similar results were obtained as in the proteomics approach, Tmem16b was robustly detected, and in addition, we detected Tmem16a, f, and k mRNAs.

### Tmem16b is expressed in the cilia of mature olfactory neurons

The Tmem16b::EGFP fusion protein was shown to traffic to olfactory cilia (Stephan et al. 2009), but the localization of the endogenous channel in the OSNs still needs to be determined. To analyze the subcellular localization, we generated an antibody against an intracellular epitope, which is unique for Tmem16b (Supplementary Figure 2). The antibody specifically stains recombinantly expressed Tmem16b in HEK293 cells, without major background staining of the untransfected cells, and detected recombinantly expressed Tmem16b by western blotting (Supplementary Figure 2). Moreover, no band was detected in tissues expressing Tmem16a, such as lung (Figure 3), indicating specificity of the antibody for Tmem16b.

Using this antibody, we could show that the protein is highly enriched in the cilia of OSNs because Tmem16b showed nearly complete colocalization in cryosections of OMP-GFP mice with marker proteins for olfactory cilia such as acetylated tubulin and CNGA2 (Figure 2A).

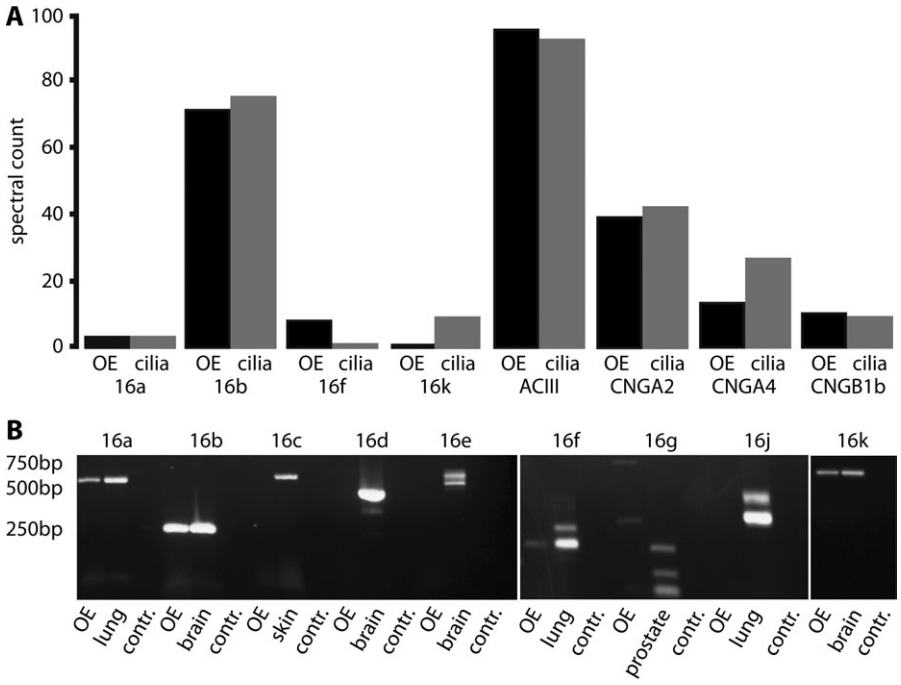


**Figure 1** Expression of Tmem16 family members in the OE. **(A)** Semiquantitative evaluation of the relative abundance of Tmem16 family members, as well as CNGA2, CNGA4, CNGB1b, and ACIII in olfactory plasma membranes (black bars) and olfactory cilia preparations (gray bars) on the basis of spectral counts, the data are contained in Supplementary Tables S1 and S2. **(B)** RT-PCR analysis of Tmem16 family member expression in the OE, different reference tissue samples and negative control (water) using intron-spanning primer pairs.

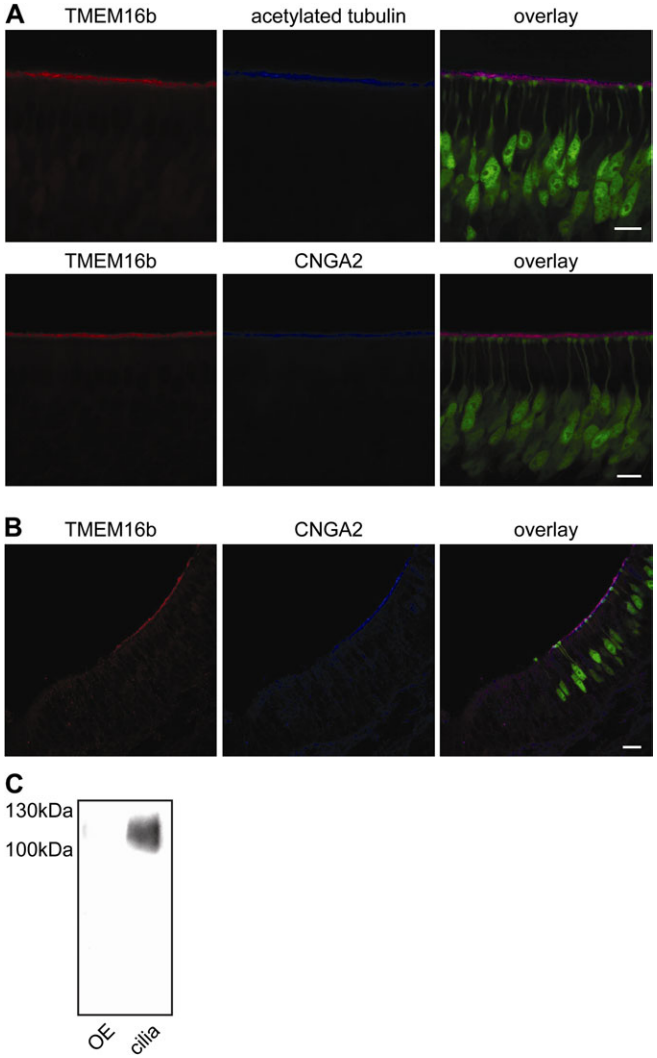


**Figure 2** Tmem16b is expressed in the cilia of OSNs. **(A)** Colocalization of Tmem16b (red) with acetylated tubulin and CNGA2 (blue) in cryosections of OMP-GFP transgenic mice, mature neurons are green in the overlay. **(B)** Tmem16b (red) and CNGA2 (blue) expression is restricted to the sensory part of the OE, in which mature neurons appear in green. **(C)** Detection of Tmem16b in membrane preparations of OE and cilia enriched fractions (cilia) by western blotting. Equal amounts of total protein were loaded in both lanes. Scale Bar = 10 μm.

Loading of equal protein amounts resulted in strong bands in the cilia fraction compared with whole OE (Figure 2C). Increased detection time also allowed the detection of the Tmem16b in lysates from complete OE (Figure 3). From western blotting we could furthermore deduce that Tmem16b seems to be highly glycosylated in the ciliary compartment (Figure 2C), which is in accordance to recent work in the retina (Stohr et al. 2009) where Tmem16b also showed diffuse banding pattern. Moreover, Tmem16b was only expressed in the sensory part of the nasal epithelium because staining was restricted to the part of the epithelium where OMP and CNGA2 positive neurons were present (Figure 2B).

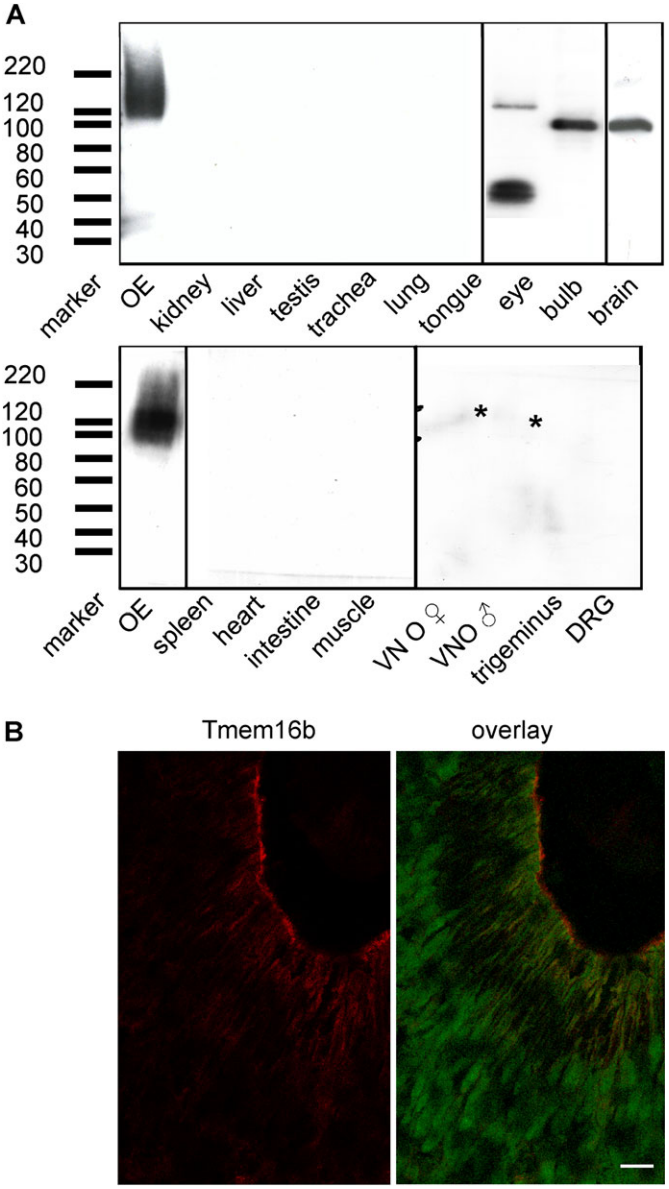


**Figure 3** Tmem16b shows highest expression level in the main OE. **(A)** Localization of Tmem16b in membrane preparations of different tissues by western blotting, equal amounts of total protein was loaded for the different tissues. Each experiment was performed at least 3 times. Asterisks denote weak bands detected in the vomeronasal organ. **(B)** Tmem16b (red) expression in the sensory microvilli of vomeronasal neurons. Scale Bar = 20 μm.

### Tmem16b is specifically expressed in the OE

Tmem16a was found in a multitude of tissues where secretory epithelial cells are present, in sensory cells and in the retina (Schroeder et al. 2008; Yang et al. 2008). We therefore determined whether Tmem16b also shows a ubiquitous expression pattern or whether expression is specific for certain tissues. Significant expression could only be detected in OE, olfactory bulb, eye, and brain. In membrane preparations of different tissues, such as kidney, liver, testis, trachea, lung, tongue, spleen, heart, intestine, and skeletal muscle we did

not detect Tmem16b in similar amounts as in the OE (Figure 3). The major band in the retina membrane preparations had only a size of approximately 50 kD, whereas the major isoform in the OE had the expected size of 110 kD. Whether the lower molecular weight isoform detected in retina presents a functional ion channel is unclear; a higher molecular weight band as reported (Stohr et al. 2009) can also be detected. Other sensory tissues do not seem to express Tmem16b because it was not detectable from trigeminal or dorsal root ganglia (Figure 3). Tmem16b can be detected in the vomeronasal organ from male and female mice, but at much lower expression levels than in the main OE (Figure 3 and Supplementary Figure 3). Immunostainings of cryosections from the vomeronasal organ showed Tmem16b expression in the sensory microvilli of the sensory neurons (Figure 3B).

## Discussion

Using semiquantitative proteomics and immunodetection we show here that Tmem16b, recently proposed as candidate CaCC in the olfactory system (Stephan et al. 2009), is present in the right amount and at the right location to fulfill its well-known function in the olfactory signal transduction cascade.

Using a highly sensitive proteomics approach allowed us to semiquantitatively analyze the membrane proteome of cilia from OSNs. Among the identified proteins were members of a novel family of CaCCs (Tmem16a, Tmem16b, Tmem16f, and Tmem16k). Although Tmem16b was detected in proteomic analysis of olfactory cilia membranes previously (Mayer et al. 2008; Stephan et al. 2009), it was unclear whether it is expressed in proper amounts to serve as CaCC in olfactory signal transduction. Performing a semiquantitative analysis of the relative abundance of membrane proteins in olfactory membranes on the basis of spectral counts (Liu et al. 2004), we found Tmem16b to be one of the most abundant membrane proteins in the OE. It is expressed in notably higher expression levels than the other Tmem16 family members. Tmem16b was found to be nearly twice as abundant as the CNGA2 subunit, and approximately 3-fold higher expressed than CNGA4 and ~8-fold higher than CNGB1b. This is consistent with the fact that the maximum $Cl^-$ current is greater than the maximum CNG current by a factor of 33 (Reisert et al. 2003). Based on physiological experiments, it was estimated that $Cl^-$ channels in rat are in excess by a factor of 8 compared with CNG channels (Reisert et al. 2003), which is in the same order of magnitude as the Tmem16b:CNGB1b ratio we found in our experiments. Tmem16b is therefore present in a proper amount in olfactory membranes to be a likely candidate as olfactory CaCC. Consistent with this estimate is our observation that the protein is readily present in the cilia of OSNs, similar as the CNGA2 channel subunit.

Functional studies on recombinantly expressed Tmem16b in HEK293 cells indicated that it encodes a CaCC (Supplementary Figure 4), consistent with previous reports showing that mouse Tmem16b gives rise to CaCC in Axolotl oocytes (Schroeder et al. 2008) and HEK293 cells (Pifferi et al. 2009; Stephan et al. 2009). A detailed comparison of recombinantly expressed Tmem16b in HEK293 cells with the endogenous CaCCs in OSNs was published recently (Stephan et al. 2009), demonstrating that the biophysical properties of the channels are very similar. Nevertheless, the remaining differences between the endogenous olfactory CaCC and heterologously expressed Tmem16b raise the possibility that Tmem16b forms complexes with other proteins in olfactory cilia. In that respect it is interesting to note that we could identify 3 other Tmem16 family members (Tmem16a, f, and k) on the protein level in our samples, which are possible interaction partners. Tmem16f and k were found to be present in similar amounts as CNG1B.

Western blotting revealed that Tmem16b expression is highly specific for the OE, the protein was not detectable in similar amounts in nearly all other tissues tested, except brain. This is in contrast to Tmem16a, which was found to be relatively ubiquitously expressed, mostly in secretory epithelial cells (Caputo et al. 2008; Schroeder et al. 2008; Yang et al. 2008). Tmem16b was recently identified in the photoreceptor synaptic terminals in mouse retina (Stohr et al. 2009), which is consistent with our detection showing expression in eye membrane preparations, but the expression level was found to be significantly lower than in the OE. Low expression levels of Tmem16b were also detected in the vomeronasal organ but not in other sensory tissues such as trigeminal and dorsal root ganglia and tongue. Tmem16b seems to be glycosylated in the cilia of the OSNs, similar as the type III adenylyl cyclase (Bakalyar and Reed 1990) and the CNGA2 subunit of the CNG channel (Bonigk et al. 1999). The functions of these glycosylations are not known to date but might be implicated in surface or ciliary trafficking of the respective proteins. Detection of the endogenous channel in OE cryosections allowed to unambiguously confirm ciliary localization in the sensory part of the nasal epithelium, where Tmem16b readily colocalized with CNGA2. Tmem16b was moreover localized in the microvilli of sensory neurons in the vomeronasal organ, which could indicate a role in signal transduction also in this tissue.

Taken together we show here that Tmem16b, the second characterized member of a new family of CaCC, is highly specific for the olfactory system and shows prominent ciliary localization in OSNs. Moreover, Tmem16b is present in adequate amounts to be the well-known CaCC in the olfactory system. Further characterization of the other members of the family that are present in OSNs will help to further refine the significance of this ion channel family in olfactory signal transduction.

## Supplementary material

Supplementary material can be found at http://www.chemse.oxfordjournals.org/.

## Funding

This work was supported by grants from the Deutsche Forschungsgemeinschaft [SFB642 to E.M.N and H.H.]; the Max-Planck-Research School for Chemical Biology; the Ruhr-University Research School; and the Heinrich und Alma Vogelsang Stiftung.

## Acknowledgements

We thank H. Bartel and J. Gerkrath for excellent technical assistance, K. Überla and M. Tenbusch (Ruhr-Universität Bochum) for help with FACS sorting, and M. Spehr (RWTH Aachen) for valuable discussions.

## References

Bakall B, McLaughlin P, Stanton JB, Zhang Y, Hartzell HC, Marmorstein LY, Marmorstein AD. 2008. Bestrophin-2 is involved in the generation of intraocular pressure. Invest Ophthalmol Vis Sci. 49:1563–1570.

Bakalyar HA, Reed RR. 1990. Identification of a specialized adenylyl cyclase that may mediate odorant detection. Science. 250:1403–1406.

Bonigk W, Bradley J, Muller F, Sesti F, Boekhoff I, Ronnett GV, Kaupp UB, Frings S. 1999. The native rat olfactory cyclic nucleotide-gated channel is composed of three distinct subunits. J Neurosci. 19:5332–5347.

Caputo A, Caci E, Ferrera L, Pedemonte N, Barsanti C, Sondo E, Pfeffer U, Ravazzolo R, Zegarra-Moran O, Galietta LJ. 2008. TMEM16A, a membrane protein associated with calcium-dependent chloride channel activity. Science. 322:590–594.

Frings S, Reuter D, Kleene SJ. 2000. Neuronal $Ca2^{+}$ -activated $Cl^{-}$ channels–homing in on an elusive channel species. Prog Neurobiol. 60:247–289.

Huang X, Godfrey TE, Gooding WE, McCarty KS Jr, Gollin SM. 2006. Comprehensive genome and transcriptome analysis of the 11q13 amplicon in human oral cancer and synteny to the 7F5 amplicon in murine oral carcinoma. Genes Chromosomes Cancer. 45:1058–1069.

Liu H, Sadygov RG, Yates JRIII. 2004. A model for random sampling and estimation of relative protein abundance in shotgun proteomics. Anal Chem. 76:4193–4201.

Mayer U, Ungerer N, Klimmeck D, Warnken U, Schnolzer M, Frings S, Mohrlen F. 2008. Proteomic analysis of a membrane preparation from rat olfactory sensory cilia. Chem Senses. 33:145–162.

Perkins DN, Pappin DJ, Creasy DM, Cottrell JS. 1999. Probability-based protein identification by searching sequence databases using mass spectrometry data. Electrophoresis. 20:3551–3567.

Pifferi S, Dibattista M, Menini A. 2009. TMEM16B induces chloride currents activated by calcium in mammalian cells. Pflugers Arch. 458: 1023–1038.

Pifferi S, Pascarella G, Boccaccio A, Mazzatenta A, Gustincich S, Menini A, Zucchelli S. 2006. Bestrophin-2 is a candidate calcium-activated chloride channel involved in olfactory transduction. Proc Natl Acad Sci U S A. 103:12929–12934.

Potter SM, Zheng C, Koos DS, Feinstein P, Fraser SE, Mombaerts P. 2001. Structure and emergence of specific olfactory glomeruli in the mouse. J Neuroscience. 21:9713–9723.

Reisert J, Bauer PJ, Yau KW, Frings S. 2003. The Ca-activated Cl channel and its control in rat olfactory receptor neurons. J Gen Physiol. 122: 349–363.

Reisert J, Lai J, Yau KW, Bradley J. 2005. Mechanism of the excitatory $Cl^{-}$ response in mouse olfactory receptor neurons. Neuron. 45:553–561.

Schaefer H, Chervet JP, Bunse C, Joppich C, Meyer HE, Marcus K. 2004. A peptide preconcentration approach for nano-high-performance liquid chromatography to diminish memory effects. Proteomics. 4:2541–2544.

Schroeder BC, Cheng T, Jan YN, Jan LY. 2008. Expression cloning of TMEM16A as a calcium-activated chloride channel subunit. Cell. 134: 1019–1029.

Stephan AB, Shum EY, Hirsh S, Cygnar KD, Reisert J, Zhao H. 2009. ANO2 is the cilial calcium-activated chloride channel that may mediate olfactory amplification. Proc Natl Acad Sci U S A. 106:11776–11781.

Stephan C, Reidegeld KA, Hamacher M, van HA, Marcus K, Taylor C, Jones P, Muller M, Apweiler R, Martens L, et al. 2006. Automated reprocessing pipeline for searching heterogeneous mass spectrometric data of the HUPO Brain Proteome Project pilot phase. Proteomics. 6:5015–5029.

Stohr H, Heisig JB, Benz PM, Schoberl S, Milenkovic VM, Strauss O, Aartsen WM, Wijnholds J, Weber BH, Schulz HL. 2009. TMEM16B, a novel protein with calcium-dependent chloride channel activity, associates with a presynaptic protein complex in photoreceptor terminals. J Neurosci. 29:6809–6818.

Tsutsumi S, Inoue H, Sakamoto Y, Mizuta K, Kamata N, Itakura M. 2005. Molecular cloning and characterization of the murine gnathodiaphyseal dysplasia gene GDD1. Biochem Biophys Res Commun. 331: 1099–1106.

Wiese S, Gronemeyer T, Ofman R, Kunze M, Grou CP, Almeida JA, Eisenacher M, Stephan C, Hayen H, Schollenberger L, et al. 2007. Proteomics characterization of mouse kidney peroxisomes by tandem mass spectrometry and protein correlation profiling. Mol Cell Proteomics. 6:2045–2057.

Yang YD, Cho H, Koo JY, Tak MH, Cho Y, Shim WS, Park SP, Lee J, Lee B, Kim BM, et al. 2008. TMEM16A confers receptor-activated calcium-dependent chloride conductance. Nature. 455:1210–1215.